

University of Wollongong Research Online

Faculty of Engineering and Information
Sciences - Papers: Part A

Faculty of Engineering and Information
Sciences

1-1-2012

Reconfigurable photonic crystal waveguides created by selective liquid infiltration

A Casas Bedoya
University of Sydney

P Domachuk
University of Sydney


C Grillet
University of Sydney

C Monat
Universite de Lyon

E Magi
University of Sydney

See next page for additional authors

Follow this and additional works at: <https://ro.uow.edu.au/eispapers>

 Part of the [Engineering Commons](#), and the [Science and Technology Studies Commons](#)

Recommended Citation

Casas Bedoya, A; Domachuk, P; Grillet, C; Monat, C; Magi, E; Li, Enbang; and Eggleton, Benjamin J., "Reconfigurable photonic crystal waveguides created by selective liquid infiltration" (2012). *Faculty of Engineering and Information Sciences - Papers: Part A*. 2866.
<https://ro.uow.edu.au/eispapers/2866>

Research Online is the open access institutional repository for the University of Wollongong. For further information contact the UOW Library: research-pubs@uow.edu.au

Reconfigurable photonic crystal waveguides created by selective liquid infiltration

Abstract

We experimentally demonstrate reconfigurable photonic crystal waveguides created directly by infiltrating high refractive index ($n \approx 2.01$) liquids into selected air holes of a two-dimensional hexagonal periodic lattice in silicon. The resulting effective index contrast is large enough that a single row of infiltrated holes enables light propagation at near-infrared wavelengths. We include a detailed comparison between modeling and experimental results of single line defect waveguides and show how our infiltration procedure is reversible and repeatable. We achieve infiltration accuracy down to the single air hole level and demonstrate control on the volume of liquid infused into the holes by simply changing the infiltration velocity. This method is promising for achieving a wide range of targeted optical functionalities on a "blank" photonic crystal membrane that can be reconfigured on demand.

Keywords

waveguides, liquid, reconfigurable, photonic, created, selective, crystal, infiltration

Disciplines

Engineering | Science and Technology Studies

Publication Details

Casas Bedoya, A., Domachuk, P., Grillet, C., Monat, C., Magi, E., Li, E. & Eggleton, B. (2012). Reconfigurable photonic crystal waveguides created by selective liquid infiltration. *Optics Express*, 20 (10), 11046-11056.

Authors

A Casas Bedoya, P Domachuk, C Grillet, C Monat, E Magi, Enbang Li, and Benjamin J. Eggleton

Reconfigurable photonic crystal waveguides created by selective liquid infiltration

A. Casas Bedoya,^{1,*} P. Domachuk,¹ C. Grillet,¹ C. Monat,² E.C. Mägi,¹ E. Li,¹ and B. J. Eggleton¹

¹Centre for Ultrahigh bandwidth Devices for Optical Systems (CUDOS), Institute of Photonics and Optical Science (IPOS), School of Physics, University of Sydney, New South Wales 2006, Australia

²Université de Lyon, Institut des Nanotechnologies de Lyon (INL)-UMR 5270, CNRS, Ecole Centrale de Lyon, Ecully, France

*casas@physics.usyd.edu.au

Abstract: We experimentally demonstrate reconfigurable photonic crystal waveguides created directly by infiltrating high refractive index ($n \approx 2.01$) liquids into selected air holes of a two-dimensional hexagonal periodic lattice in silicon. The resulting effective index contrast is large enough that a single row of infiltrated holes enables light propagation at near-infrared wavelengths. We include a detailed comparison between modeling and experimental results of single line defect waveguides and show how our infiltration procedure is reversible and repeatable. We achieve infiltration accuracy down to the single air hole level and demonstrate control on the volume of liquid infused into the holes by simply changing the infiltration velocity. This method is promising for achieving a wide range of targeted optical functionalities on a “blank” photonic crystal membrane that can be reconfigured on demand.

©2012 Optical Society of America

OCIS codes: (230.5298) Photonic crystals; (130.5296) Photonic crystal waveguides; (350.4238) Nanophotonics and photonic crystals; (250.5300) Photonic integrated circuits.

References and links

1. T. F. Krauss, R. M. DeLaRue, and S. Brand, “Two-dimensional photonic-bandgap structures operating at near infrared wavelengths,” *Nature* **383**(6602), 699–702 (1996).
2. S. Y. Lin, E. Chow, S. G. Johnson, P. R. Villeneuve, J. D. Joannopoulos, J. R. Wendt, G. A. Vawter, W. Zubrzycki, H. Hou, and A. Alleman, “Three-dimensional control of light in a two-dimensional photonic crystal slab,” *Nature* **407**(6807), 983–986 (2000).
3. D. Freeman, C. Grillet, M. W. Lee, C. L. C. Smith, Y. Ruan, A. Rode, M. Krolikowska, S. Tomljenovic-Hanic, M. de Sterke, M. J. Steel, B. Luther-Davies, S. Madden, D. J. Moss, Y. H. Lee, and B. J. Eggleton, “Chalcogenide glass photonic crystals,” *Photonics Nanostruct. Fundam. Appl.* **6**(1), 3–11 (2008).
4. D. Freeman, S. Madden, and B. Luther-Davies, “Fabrication of planar photonic crystals in a chalcogenide glass using a focused ion beam,” *Opt. Express* **13**(8), 3079–3086 (2005).
5. Y. Akahane, T. Asano, B. S. Song, and S. Noda, “High-Q photonic nanocavity in a two-dimensional photonic crystal,” *Nature* **425**(6961), 944–947 (2003).
6. T. Baba, “Slow light in photonic crystals,” *Nat. Photonics* **2**(8), 465–473 (2008).
7. M. Ebnali-Heidari, C. Grillet, C. Monat, and B. J. Eggleton, “Dispersion engineering of slow light photonic crystal waveguides using microfluidic infiltration,” *Opt. Express* **17**(3), 1628–1635 (2009).
8. C. Monat, B. Corcoran, M. Ebnali-Heidari, C. Grillet, B. J. Eggleton, T. P. White, L. O’Faolain, and T. F. Krauss, “Slow light enhancement of nonlinear effects in silicon engineered photonic crystal waveguides,” *Opt. Express* **17**(4), 2944–2953 (2009).
9. B. Corcoran, C. Monat, M. Pelusi, C. Grillet, T. P. White, L. O’Faolain, T. F. Krauss, B. J. Eggleton, and D. J. Moss, “Optical signal processing on a silicon chip at 640Gb/s using slow-light,” *Opt. Express* **18**(8), 7770–7781 (2010).
10. C. Grillet, C. Monat, C. L. Smith, M. W. Lee, S. Tomljenovic-Hanic, C. Karnutsch, and B. J. Eggleton, “Reconfigurable photonic crystal circuits,” *Laser Photonics Rev.* **4**(2), 192–204 (2010).
11. M. W. Lee, C. Grillet, C. Monat, E. Mägi, S. Tomljenovic-Hanic, X. Gai, S. Madden, D. Y. Choi, D. Bulla, B. Luther-Davies, and B. J. Eggleton, “Photosensitive and thermal nonlinear effects in chalcogenide photonic crystal cavities,” *Opt. Express* **18**(25), 26695–26703 (2010).

12. I. Märki, M. Salt, and H. P. Herzig, "Tuning the resonance of a photonic crystal microcavity with an AFM probe," *Opt. Express* **14**(7), 2969–2978 (2006).
13. K. Busch and S. John, "Liquid-Crystal photonic-band-gap materials: The tunable electromagnetic vacuum," *Phys. Rev. Lett.* **83**(5), 967–970 (1999).
14. S. W. Leonard, J. P. Mondia, H. M. van Driel, O. Toader, S. John, K. Busch, A. Birner, U. Gosele, and V. Lehmann, "Tunable two-dimensional photonic crystals using liquid-crystal infiltration," *Phys. Rev. B* **61**(4), R2389–R2392 (2000).
15. C. Schuller, F. Klopff, J. P. Reithmaier, M. Kamp, and A. Forchel, "Tunable photonic crystals fabricated in III-V semiconductor slab waveguides using infiltrated liquid crystals," *Appl. Phys. Lett.* **82**(17), 2767–2769 (2003).
16. B. Maune, M. Loncar, J. Witzens, M. Hochberg, T. Baehr-Jones, D. Psaltis, A. Scherer, and Y. M. Qiu, "Liquid-crystal electric tuning of a photonic crystal laser," *Appl. Phys. Lett.* **85**(3), 360–362 (2004).
17. C. Monat, P. Domachuk, C. Grillet, M. Collins, B. J. Eggleton, M. Cronin-Golomb, S. Mutzenich, T. Mahmud, G. Rosengarten, and A. Mitchell, "Optofluidics: a novel generation of reconfigurable and adaptive compact architectures," in *Microfluid Nanofluid* (Springer-Verlag, 2007), pp. 81–95.
18. D. Psaltis, S. R. Quake, and C. H. Yang, "Developing optofluidic technology through the fusion of microfluidics and optics," *Nature* **442**(7101), 381–386 (2006).
19. C. Monat, P. Domachuk, and B. J. Eggleton, "Integrated optofluidics: A new river of light," *Nat. Photonics* **1**(2), 106–114 (2007).
20. A. Casas Bedoya, S. Mahmoodian, C. Monat, S. Tomljenovic-Hanic, C. Grillet, P. Domachuk, E. C. Mägi, B. J. Eggleton, and R. W. van der Heijden, "Liquid crystal dynamics in a photonic crystal cavity created by selective microfluidic infiltration," *Opt. Express* **18**(26), 27280–27290 (2010).
21. C. L. C. Smith, U. Bog, S. Tomljenovic-Hanic, M. W. Lee, D. K. C. Wu, L. O'Faolain, C. Monat, C. Grillet, T. F. Krauss, C. Karnutsch, R. C. McPhedran, and B. J. Eggleton, "Reconfigurable microfluidic photonic crystal slab cavities," *Opt. Express* **16**(20), 15887–15896 (2008).
22. F. Intonti, S. Vignolini, V. Türeci, M. Colocci, P. Bettotti, L. Pavesi, S. L. Schweizer, R. Wehrspohn, and D. Wiersma, "Rewritable photonic circuits," *Appl. Phys. Lett.* **89**(21), 211117 (2006).
23. D. Erickson, T. Rockwood, T. Emery, A. Scherer, and D. Psaltis, "Nanofluidic tuning of photonic crystal circuits," *Opt. Lett.* **31**(1), 59–61 (2006).
24. F. Intonti, S. Vignolini, F. Riboli, M. Zani, D. S. Wiersma, L. Balet, L. H. Li, M. Francardi, A. Gerardino, A. Fiore, and M. Gurioli, "Tuning of photonic crystal cavities by controlled removal of locally infiltrated water," *Appl. Phys. Lett.* **95**(17), 173112 (2009).
25. S. F. Mingaleev, M. Schillinger, D. Hermann, and K. Busch, "Tunable photonic crystal circuits: concepts and designs based on single-pore infiltration," *Opt. Lett.* **29**(24), 2858–2860 (2004).
26. H. Kurt and D. S. Citrin, "Reconfigurable multimode photonic-crystal waveguides," *Opt. Express* **16**(16), 11995–12001 (2008).
27. S. Tomljenovic-Hanic, C. M. de Sterke, and M. J. Steel, "Design of high-Q cavities in photonic crystal slab heterostructures by air-holes infiltration," *Opt. Express* **14**(25), 12451–12456 (2006).
28. C. L. C. Smith, D. K. C. Wu, M. W. Lee, C. Monat, S. Tomljenovic-Hanic, C. Grillet, B. J. Eggleton, D. Freeman, Y. Ruan, S. Madden, B. Luther-Davies, H. Giessen, and Y.-H. Lee, "Microfluidic photonic crystal double heterostructures," *Appl. Phys. Lett.* **91**(12), 121103 (2007).
29. U. Bog, C. L. C. Smith, M. W. Lee, S. Tomljenovic-Hanic, C. Grillet, C. Monat, L. O'Faolain, C. Karnutsch, T. F. Krauss, R. C. McPhedran, and B. J. Eggleton, "High-Q microfluidic cavities in silicon-based two-dimensional photonic crystal structures," *Opt. Lett.* **33**(19), 2206–2208 (2008).
30. E. Yablonovitch, "Optics: Liquid versus photonic crystals," *Nature* **401**(6753), 539–541 (1999).
31. The European FP6 Network of Excellence for photonic integrated components and circuits, <http://www.epixnet.org>
32. A. C. Bedoya, C. Monat, P. Domachuk, C. Grillet, and B. J. Eggleton, "Measuring the dispersive properties of liquids using a microinterferometer," *Appl. Opt.* **50**(16), 2408–2412 (2011).
33. A. F. Stalder, G. Kulik, D. Sage, L. Barbieri, and P. Hoffmann, "A Snake-Based Approach to Accurate Determination of Both Contact Points and Contact Angles," *Colloids Surf. A Physicochem. Eng. Asp.* **286**(1-3), 92–103 (2006).
34. C. Grillet, P. Domachuk, V. Ta'eed, E. Mägi, J. A. Bolger, B. J. Eggleton, L. Rodd, and J. Cooper-White, "Compact tunable microfluidic interferometer," *Opt. Express* **12**(22), 5440–5447 (2004).
35. RSoft Inc, RSoft Fullwave FDTD code, <http://www.rsoftdesign.com>.
36. B. S. Song, T. Asano, Y. Akahane, Y. Tanaka, and S. Noda, "Transmission and reflection characteristics of in-plane hetero-photonic crystals," *Appl. Phys. Lett.* **85**(20), 4591–4593 (2004).
37. D. O'Brien, M. D. Settle, T. Karle, A. Michaeli, M. Salib, and T. F. Krauss, "Coupled photonic crystal heterostructure nanocavities," *Opt. Express* **15**(3), 1228–1233 (2007).
38. T. Tanabe, M. Notomi, E. Kuramochi, A. Shinya, and H. Taniyama, "Trapping and delaying photons for one nanosecond in an ultrasmall high-Q photonic-crystal nanocavity," *Nat. Photonics* **1**(1), 49–52 (2007).
39. B. S. Song, S. Noda, T. Asano, and Y. Akahane, "Ultra-high-Q photonic double-heterostructure nanocavity," *Nat. Mater.* **4**(3), 207–210 (2005).
40. M. Notomi, E. Kuramochi, and T. Tanabe, "Large-scale arrays of ultrahigh-Q coupled nanocavities," *Nat. Photonics* **2**(12), 741–747 (2008).

1. Introduction

Photonic crystals (PhC) are an attractive platform for the development of compact optical devices. In particular planar PhCs formed by a two-dimensional periodic array of air holes in a submicron dielectric slab, can control light on the wavelength scale [1,2]. These structures are commonly fabricated with lithographic techniques and the optical functions are obtained by perfectly positioning air sub-micron air holes within a high refractive index material [1,2], generally silicon, III-V semiconductors, and more recently chalcogenide glass [3,4]. Two key building blocks to create complex and advanced functionalities on PhCs are cavities and waveguides. These are typically created through managing point [5] and linear defects [6] in the PhC lattice during fabrication. Depending upon their design, PhC waveguides allow single mode propagation at particular frequencies. The main advantage and the fundamental difference with nanowires is their highly dispersive nature, which can be engineered [7,8]; for instance slow light regimes can be achieved over wide bandwidths [6], which is critical for enhancing light-matter interaction for high bit rate optical signals [9].

Due to the removal of material to form the periodic voids, lithographic fabrication limits the reconfigurability and tunability of the resulting PhC devices [10]. Some approaches based on thermal, electrical, or mechanical tuning [10–12] have been demonstrated to overcome this limitation. The infiltration of liquids into the PhC air voids, referred to as optofluidic tuning, has been long suggested [13] and demonstrated [14–16], providing in principle a much wider tuning range [17]. Optofluidics [18,19], the combination of microfluidics and microphotronics, is especially effective in tuning photonic structures, through the infiltration of a wide variety of liquids with refractive indices ranging between 1.3 and 2 giving potentially, more widely tunable optical properties than semiconductors (see e.g. liquid crystals [14–16,20]). This degree of freedom in the liquid choice combined with the reversibility of the infiltration process [21,22] makes optofluidic tuning a flexible, efficient and versatile method for post-engineering and reconfiguring PhC architectures [7,23,24].

In addition to using liquids to tune pre-existing PhC cavities or waveguides, the idea has been proposed to directly create optical functions by infiltrating liquids into an otherwise regular PhC area [13,25–27]. Local liquid infiltration has been experimentally applied to the creation of photonic crystal cavities [20,21,28,29]. However, both the large effective index contrast and high level of accuracy required to create a PhC waveguide through infiltrating a single row of holes has thus far prevented such a demonstration. Apart from a fine control on the infiltration process, one of the main factors influencing the selective PhC infiltration, as expressed by Eli Yablonovitch [30] a decade ago, is the angle formed between the liquid and the material surface, i.e. the contact angle. This physical condition imposes a restriction on the amount of liquid to be infiltrated, affecting directly the effective refractive index changes afforded by the infiltration and adding an extra challenge [26] to the creation of PhC waveguides based on single row infiltration.

In this work we demonstrate experimentally how PhC waveguides can be directly created by selectively infiltrating high refractive index liquids into the air holes of a two dimensional silicon PhC periodic lattice. The resulting effective index contrast achieved by infiltration is large enough that a single row of infiltrated air holes allows light propagation, i.e. effectively creating a single line waveguide in an otherwise “blank” and reflective PhC. Due to the mobile nature of the infused liquid, the optofluidic PhC waveguides created are intrinsically reconfigurable. This approach also offers the possibility of creating more complex reconfigurable photonic circuits (e.g. including optofluidic waveguides and cavities). Our technique not only allows for the infiltration of selected air holes (position and number) with a relatively high accuracy, almost down to the single hole level, but it also enables us to control the volume of liquid introduced into the holes, through varying the “writing” speed during the infiltration process. Combined with the use of high index liquids, this controlled infiltration technique gives us an additional degree of freedom for achieving the desired optical

functionality. In section two; we describe the fabricated structures used for this work. In section three, we explain the selective infiltration process, how the liquid behaves inside the PhC sub-micrometric holes and its consequences, and in sections four and five, we explain and discuss the experimental results and different possibilities that can be explored using the selective infiltration technique.

2. Fabrication of the silicon photonic crystal membranes

The photonic crystals were fabricated on Silicon-on-Insulator (SOI) under the EPIXnet Framework [31]. 193nm deep UV lithography and Reactive Ion Etching (RIE) were used to create the PhC holes into the 220nm thick Si membrane. To remove the silica sacrificial layer under the Si slab, we first used a positive photoresist to expose a square mask with the size of the PhC array to protect the waveguides and to open space for the wet etching process; we then under etched the sample by immersing it during 16 minutes in a buffered HF (5:1) solution.

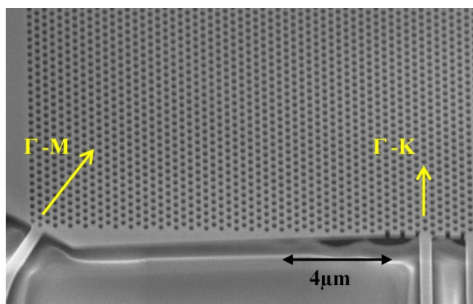


Fig. 1. Scanning Electron Microscopy (SEM) picture of the fabricated airbridged PhC membrane, with input waveguides in the Γ -K and Γ -M directions. (Output waveguides not shown).

Figure 1 shows a Scanning Electron Microscopy (SEM) picture of the resulting air bridged PhC. The chip includes a series of PhC membranes. They consist of a regular triangular lattice of air holes with period $a = 390\text{nm}$, air hole radius $R = 0.32a$, and various lengths of 10, 20 and 60 μm along the Γ -K direction. To couple light into the PhC, we incorporated two inputs and output access nanowire waveguides along the Γ -K (0°) and Γ -M (30°) direction, as shown by the yellow arrows on Fig. 1. These waveguides are terminated at both chip end facets by cleaved waveguides of 8 μm width.

3. Selective infiltration of photonic crystals

Our selective infiltration method (see Fig. 2), relies on a micropipette with 500 nm outer diameter tip that is computer controlled by a 3 axis Eppendorf TransferMan NK 2 micromanipulator with a resolution of approximately 40 nm per actuator step. This combination makes selective infiltration a powerful and very precise technique to locally modify the refractive index of a PhC [21,24] with hole diameters of $\sim 300\text{nm}$. For the infiltration, we used the ionic liquid 1-ethyl-3-methylimidazolium heptafluoroborate. This liquid is stable at room temperature and is attractive for optofluidic applications due to its negligible vapour pressure and high refractive index, up to approximately 2.01, as was recently measured at near-IR wavelengths [32].

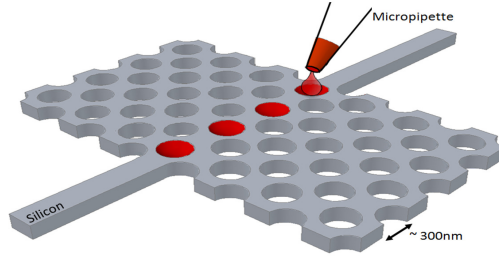


Fig. 2. 3D Schematic representation of the creation of a PhC waveguide using a selective infiltration method.

3.1 Influence of the liquid/ solid contact angle on the infiltration of photonic crystals

One of the main factors influencing the selective infiltration is the contact angle from the surface tension created between the liquid and the sample surface. This physical phenomenon imposes an upper bound on the amount of liquid that can be infiltrated into the air pores. This sets a maximum effective index modification achievable, i.e. less than the liquid refractive index.

Adding a single drop of ionic liquid on top of a silicon surface [Fig. 3 (Top-right)] and using the method presented in [33] we measured at room temperature the associated contact angle θ as the average of the two correspondent angles: $\theta_R = 61.5^\circ$ and $\theta_L = 63.2^\circ$. If we call L_t the thickness of the PhC slab and R the radius of the PhC air holes, the total volume of liquid infiltrated into a single PhC hole can be calculated by subtracting out of the hole volume ($L_t \cdot \pi \cdot R^2$), the volume of two semi spheres created at both sides of the liquid, as represented on Fig. 3. This semi sphere volume is proportional to the contact angle θ and is given by the volume integral in Eq. (1). Thus, we calculate that the maximum amount of liquid that can be infiltrated (V_h) is $\sim 75\%$ of the total hole volume.

$$V_h = L_t \cdot \pi \cdot R^2 - 2 \int_{R \cdot \cot(\theta)}^{R \cdot \csc(\theta)} \int_0^{2\pi} \int_0^\theta R^2 \cdot \sin(\theta) d\theta d\phi dR. \quad (1)$$

Although it is not possible to overcome this 75% for this particular ionic liquid/ Si slab combination, we found that propelling the pipette with higher speeds can reduce this value, as explained in section 4.

Figure 3 shows a 3D schematic representation of the shape likely to be adopted by the liquid under the contact angle influence in the symmetric PhC slab suspended in air. The origin of this curvature is the hydrophilic nature of the silicon/ ionic liquid surface. Although not attempted here, it is possible to modify this surface interaction by applying surface chemistry as was previously demonstrated [34].

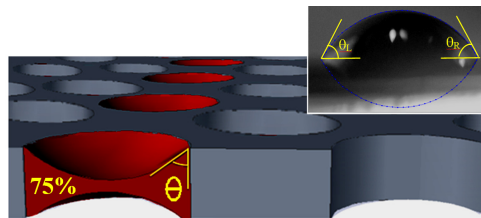


Fig. 3. 3D Schematic representation of an infiltrated PhC highlighting the contact angle (θ) and the meniscus shape adopted by the liquid. (Top-right) Contact angle picture for the ionic liquid 1-ethyl-3-methylimidazolium heptafluoroborate, on top of a Silicon surface.

The liquid is drawn first, directly into the micropipette via capillary forces by inserting the pipette into the liquid. Capillary force alone is sufficient to draw enough liquid into the pipette when its tip is brought into contact with a drop of ionic liquid. Capillary action is, then, again used to infiltrate the PhC holes while moving the pipette, now filled with liquid, across the top

of the targeted PhC area. The liquid remains suspended within the infiltrated holes due to the fluid surface tension [21].

Figure 4(a) shows a SEM picture of an infiltrated single row of PhC holes (top) surrounded by a non-infiltrated row of holes (bottom). Fig. 4(b) shows the associated intensity profiles of the image across the hole diameter, respectively performed on an infiltrated and un-infiltrated hole [red dotted lines in Fig. 4(a)]. The comparison of the intensity profiles, exhibiting a more gradual variation for the infiltrated hole, suggests that the liquid takes a meniscus shape inside the hole. Furthermore this picture also demonstrates the high liquid stability inside the holes even at pressures below 2×10^{-6} Torr in the SEM chamber.

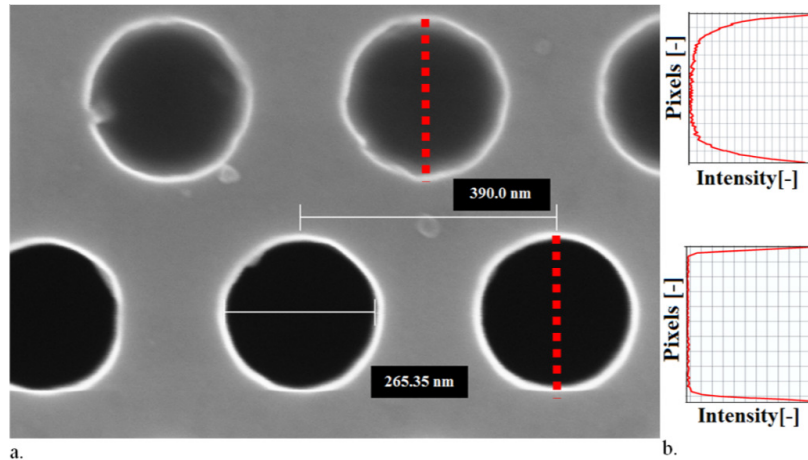


Fig. 4. (a). SEM picture of a PhC with infiltrated holes (top) vs. non-infiltrated holes (bottom). (b) Intensity profile for the infiltrated and un-infiltrated PhC holes extracted from the cross sectional SEM image (red dotted lines).

3.2 Creation of W1 liquid photonic crystal waveguides through selective liquid infiltration

In PhC architectures, leaving one row of holes out of the periodicity creates a linear defect that allows light transport with single mode propagation over a certain frequency range; this configuration is well known as a W1 PhC waveguide. In this work we realize a waveguide with a geometry close to a W1, where the refractive index of a single row of holes along the Γ -K direction of a triangular PhC lattice is modified by selective liquid infiltration. We will refer to these waveguides as W1 liquid PhC waveguides.

To obtain a mechanically stable infiltration procedure, where the correct amount of liquid is delivered into the targeted row of holes, we use a micropipette that is manipulated and aligned with respect to the PhC by the micromanipulator described earlier. In order to avoid liquid flooding the lattice, a robotic arm is used to exert the appropriate amount of pressure when displacing the filled pipette.

We were able to control the amount of infused liquid, i.e. the effective refractive index of the infiltrated PhC structures [30], by modifying the pipette actuation speed during the infiltration process. Figure 5 shows the microscope images of two liquid infiltrated PhC waveguides successively created within the same $20 \mu\text{m}$ long PhC membrane, using a slightly different infiltration procedure. For the first infiltration [Fig. 5(a)] we robotically moved the pipette filled with the ionic liquid $[\text{C}_2\text{mim}][\text{I}_7]$, at $10 \mu\text{m/s}$. Note that the infiltrated waveguide written in this case was unintentionally slightly off-centered.

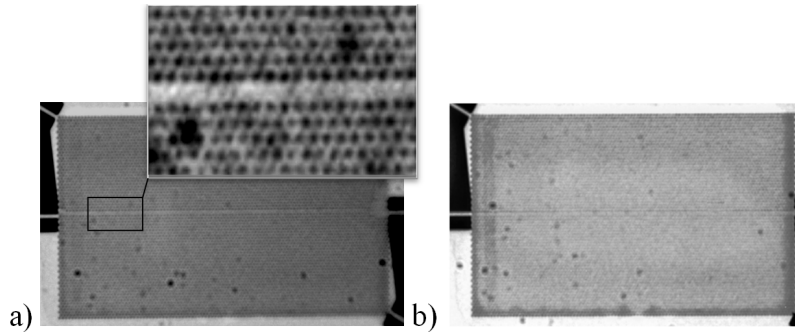


Fig. 5. Microscope picture for a 20 μm W1 PhC liquid waveguide, created using a micropipette speed of: (a) 10 $\mu\text{m}/\text{s}$. (Inset) Close up of the infiltrated central section to distinguish the single hole infiltration (b) 15 $\mu\text{m}/\text{s}$.

After the waveguide characterization we cleaned the sample by immersing it in an isopropanol bath for 1 minute. We repeated the infiltration process, but using an increased pipette actuation velocity to 15 $\mu\text{m}/\text{s}$. The waveguide thus created corresponds to a single infiltrated row perfectly aligned, in this case, with the access waveguides [see Fig. 5(b)]. As another example, we infiltrated a 60 μm long PhC membrane using the same infiltration velocity as for Fig. 5(a) (10 $\mu\text{m}/\text{s}$). The resulting infiltrated waveguide is partially displayed on Fig. 6 using a 150X objective. These different realizations demonstrate the relatively high accuracy of the infiltration procedure, and its repeatability for reaching single line infiltration at a specific location, and for different actuation speeds. We characterize all structures and describe the influence of the infiltration velocity in the incoming section.

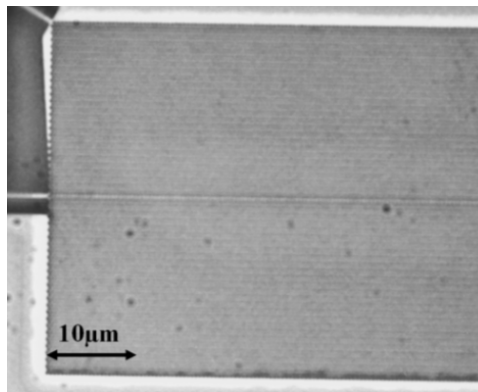


Fig. 6. Microscope picture for a 60 μm (not shown completely) W1 PhC liquid waveguide, created using a pipette speed of 10 $\mu\text{m}/\text{s}$.

4. Transmission measurements of the W1 liquid PhC waveguides and impact of the infiltration rate

The photonic band gap for the TE-like modes (E field lying mainly in the slab) of all the PhC membranes used in this work is between 1050nm and 1700nm. To characterize those structures, we used a supercontinuum photonic crystal fiber (SC 1040) as a broadband input light source. The input pulses were generated from a JDS Uniphase microchip laser (NP-10620-100) with 60mW average power. Light was butt-coupled into the chip using lensed fibers with 9dB losses per facet. The transmission spectrum was obtained using an OSA with dBm/10nm power density to resolve the maximum transmission over the entire spectrum.

We first characterized the PhC waveguides presented on Fig. 5(a) and 6, with light coupled from the left hand side. The experimental transmission spectra are plotted in Fig.

7(a), and compared with the theoretical dispersion diagram (Left) calculated for a partially infiltrated PhC (75%) using a commercial 3D plane wave expansion method solver [35]. On this diagram the green line represents the light line, the red lines correspond to the PhC bulk modes and the blue lines are the symmetric (solid) and antisymmetric (dotted line) waveguide modes. The experimental transmission spectrum (right) of the uninfiltrated PhC is also shown in red for comparison. In this case, no waveguide modes are visible within the photonic bandgap ranging between 1050nm and 1700nm; however, coupling to the bulk PhC modes was measured at lower frequencies in good agreement with the valence band of the simulated dispersion diagram. We do not observe the signature of the conduction band at high frequencies because we start approaching the silicon absorption region below 1050nm.

The dark-blue line of Fig. 7(a) represents the transmission spectrum for the 20 μm long infiltrated W1 liquid PhC waveguide of Fig. 5(a), created with a 10 $\mu\text{m/s}$ pipette velocity. Besides the coupling to the bulk PhC modes, we observe two additional transmission bands with cut-off wavelengths corresponding to 1210 and 1290 nm. Through comparing with the calculated band diagram, we can easily identify these peaks as the result of the coupling to the fundamental symmetric waveguide mode and the first higher order mode (antisymmetric).

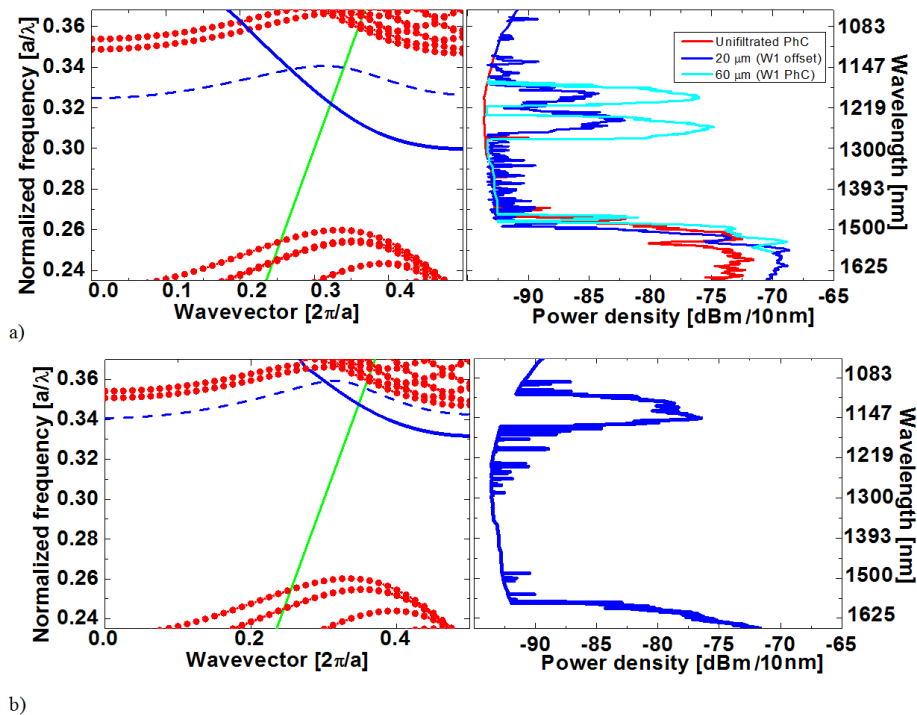


Fig. 7. (Left) Simulated dispersion diagram for a W1 liquid infiltrated PhC waveguide with period $a = 390\text{nm}$, $r = 0.32a$ and refractive index $n_{\text{IL}} = 2.01$ with a filling fraction of liquid into the holes of (a) 75% and (b) 40%. The insets show schematic representations of liquid associated waveguides, where different effective refractive indices have been represented by different colours. (Right) Experimental transmission spectrum for the different W1 liquid PhC waveguides shown on Fig. 5(a,b) and Fig. 6, i.e. (a) 20 μm (Dark blue) and 60 μm long PhC membranes (light-blue) infiltrated at 10 $\mu\text{m/s}$ and for (b) 20 μm PhC membrane infiltrated at 15 $\mu\text{m/s}$.

The experimental transmission spectrum for the 60 μm long W1 liquid PhC waveguide of Fig. 6 is also plotted on Fig. 7(a) (light-blue). Similarly to the 20 μm long W1 liquid PhC waveguide, two transmission bands are observed within the PhC photonic bandgap, and at the same spectral position. The reduction of the absolute transmission for the shorter waveguide is due to the slight offset of the infiltrated PhC waveguide with respect to the access

waveguides, as shown on Fig. 5(a). However, the cut-off wavelength for both W1 liquid PhC waveguides is 1300nm, confirming the repeatability of the infiltration procedure for the two different realizations, and the degree of control afforded by the pipette actuation speed, which was the same (10 μ m/s) for these two structures.

Considering the conservation of mass and assuming a constant flow from the pipette, it stands to reason that the faster the pipette is propelled, the less liquid it leaves in behind each hole. This reasonable assumption is confirmed through comparing the spectral signature of the 20 μ m long W1 liquid PhC waveguide created using a pipette velocity of 10 μ m/s and 15 μ m/s, respectively. The measured transmission of the latter waveguide [Fig. 5(b)] is displayed on Fig. 7(b). We observe that the transmission band associated with the waveguide modes is shifted towards higher frequencies as compared with the results of Fig. 7(a), implying a decrease in the refractive index contrast with respect to the first infiltrated waveguide. In fact, a further confirmation of the reduction in the volume of liquid inside the PhC holes is given by comparing the results of Fig. 7(b) with the dispersion diagram of a partially infiltrated PhC single line waveguide with a 40% filling fraction of liquid into the holes. This value was estimated based on the cut-off wavelength of the infiltrated waveguide measured in this case (1200nm).

In all these experiments, we found that controlling the pipette velocity and reducing its speed dramatically influences the infiltration outcome and the refractive index modification, making it possible to create reconfigurable structures with a higher degree of control. Based on this idea, we propose in the next section a different way to create photonic crystal cavities through selectively and locally varying the amount of liquid infiltrated into the PhC.

5. Selective infiltration technique for creating more complex optical functions

To explore in detail the consequences of varying the infiltration rate, we cleaned and infiltrated the same 60 μ m PhC membrane used previously, with the minimum pipette velocity afforded by our setup, i.e. 1 μ m/s. More liquid is then released from the pipette and due to capillary forces, the liquid is forced to go into the two holes adjacent to the infiltration path. The created structure, a waveguide defined by two infiltrated rows is partially shown in Fig. 8, and will be called a W2 liquid PhC waveguide.

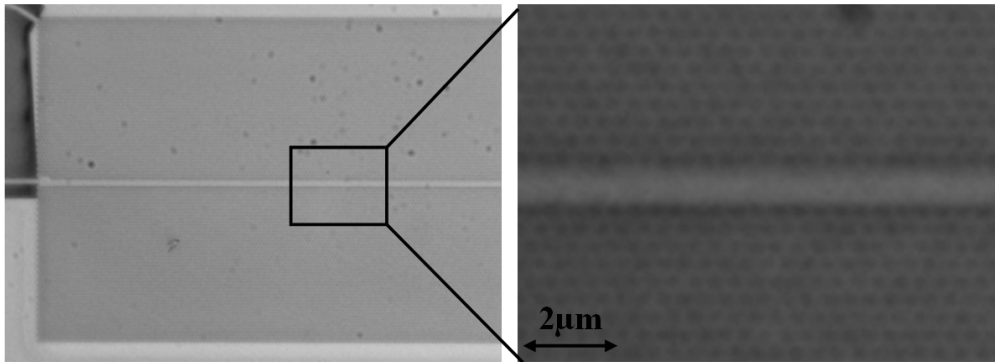


Fig. 8. Microscope picture of a 60 μ m-W2 PhC liquid waveguide, with a zoomed region demarked by a black square.

Figure 9 plots the dispersion diagram for a 75% infiltrated W2 liquid waveguide (red) and a 75% infiltrated W1 liquid waveguide (blue), previously discussed in Fig. 7(a). The experimental transmission spectrum for the infiltrated PhC membrane presented on Fig. 8 is compared in the right hand side in red. This W2 liquid waveguide spectrum exhibits coupling to the propagating modes inside the photonic bandgap between 1080 and 1460nm.

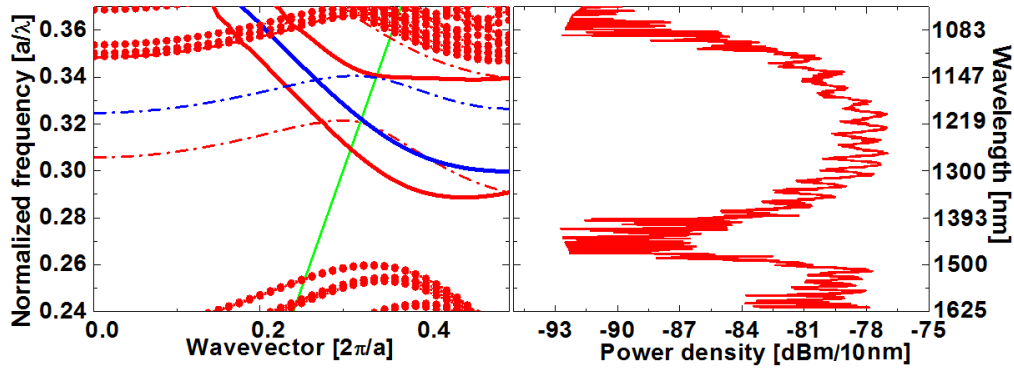


Fig. 9. (Left) Simulated dispersion diagram for a maximum infiltrated PhC waveguide W2 (Red) and W1 (Blue), with period $a = 390\text{nm}$, $r = 0.325a$ and $n_L = 2.01$. (Right) Experimental transmission spectrum for the structures presented in Fig. 8.

The possibility of obtaining a complete and reconfigurable photonic circuit can now be explored by combining different infiltration velocities. Using this concept, we propose a new way to trap light inside the PhC. We vary the infiltration velocity while infusing the liquid across the membrane, creating what is known as a heterostructure cavity [5]. Here the pipette was moved on top of the $10\mu\text{m}$ long PhC membrane, our shortest PhC sample, with different velocities: the first $3\mu\text{m}$ were crossed by the pipette at $10\mu\text{m/s}$, therefore infusing a single row of holes, the cavity formed by a two row infiltrated region was then created by reducing the velocity at $1\mu\text{m/s}$ for $2\mu\text{m}$ and finally the infiltration is speed up again to $10\mu\text{m/s}$ for the remaining $5\mu\text{m}$ of the PhC membrane. The resulting structure is presented below in Fig. 10.

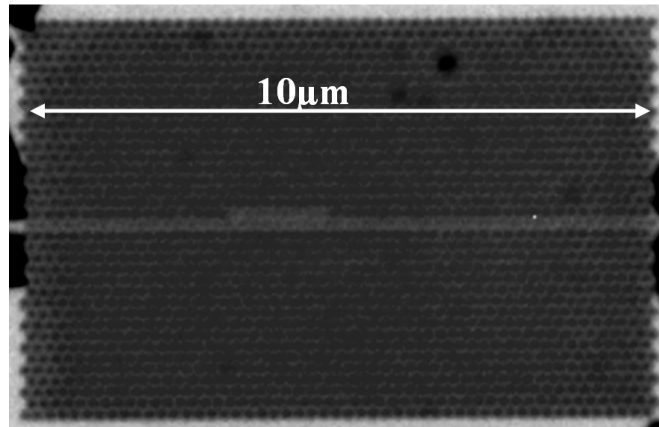


Fig. 10. $10\mu\text{m}$ PhC membrane with a heterostructure cavity created by a velocity controlled selective infiltration.

It is not possible to measure the experimental transmission of this geometry with our current setup, a butt-coupled characterization system, because as observed on the band diagram (Fig. 9), the fundamental guided mode of the W2 liquid waveguide (red) is shifted towards lower frequencies with respect to that of the W1 liquid access waveguides (blue). This creates a “mode gap” between the fundamental mode of the W1 and W2 liquid waveguides. It is at the origin of the optical confinement locally provided by the short W2 liquid section surrounded by the W1 liquid waveguides, which acts here as a PhC heterostructure cavity [5,27,28]. Conversely, this also prevents us from exciting the associated cavity modes through the W1 liquid access waveguides because these modes lie within the mode-gap.

The proposed selective infiltration technique and the design of linear defects will potentially allow us to create more complex reconfigurable photonic circuits, including, for instance, in-plane hetero-photonic crystals [36], coupled PhC heterostructure nanocavities [37–39], or even large-scale arrays of coupled nanocavities [40].

6. Conclusion

We have experimentally demonstrated how reconfigurable PhC waveguides can be created by selectively infiltrating one or two rows of holes in a silicon PhC reflective membrane with ionic liquids. This demonstration was enabled by the improvement in the infiltration technique accuracy, in terms of position and number of infused holes, as well as by the use of liquids with a high refractive index of ~ 2 . The same sets of PhC membranes were used several times, demonstrating that the technique is robust, repeatable and creates reconfigurable structures.

We have described the consequences arising from the liquid – silicon interaction. We introduced a model based on the liquid contact angle on the silicon surface to calculate the amount of liquid that can be infiltrated inside the PhC hole. The measured transmission spectra of the infiltrated waveguides were compared with 3D theoretical dispersion diagrams, showing good agreement when considering the amount of liquid infused into the holes and inferred from the model. Finally we showed how a variation of the infiltration velocity combined with a fine control of the pipette actuation make it possible to modify locally the refractive index of the PhC membrane. Due to this high degree of control and accuracy, the selective infiltration approach is promising for achieving a wide range of targeted optical functionalities within a single PhC membrane that can be reconfigured on demand.

Acknowledgments

This work was supported by an Australian Research Council (ARC) under the ARC Centres of Excellences and federation fellowships. We also acknowledge the fabrication of the SOI photonic crystals which were done in the framework of the ePIXnet Nanostructuring Platform for Photonic Integration (see <http://www.epixnet.org>). All the SEM pictures and post processing were realized at the University of New South Wales (UNSW) one of the Australian nanofabrication Facilities (ANFF) and the mask was fabricated at the Bandwidth Foundry International Pty Ltd (BFI).